Callose deposition at plasmodesmata suggests a role in viral movement restriction in transgenic tobacco plants during recovery from *Tobacco etch virus* infection

Pablo Vargas-Mejía[abg], Alejandro Olguín-Lamas[a], Selene L. Fernandez-Valverde[cdef], Carmen M. Flores-García[b], Gertrud Lund[a], Jean-Philippe Vielle-Calzada[c], and Laura Silva-Rosales[a]*

[a] Departamento de Ingeniería Genética, Centro de Investigaciones y de Estudios Avanzados, Unidad Irapuato, Guanajuato, Mexico

[b] Laboratory of AgroGenomic Sciences, Universidad Nacional Autónoma de México, León, Guanajuato, Mexico

[c] Unidad de Genómica Avanzada, Cinvestav, Irapuato, Guanajuato, Mexico.

[d] Present address: School of Biotechnology and Biomolecular Sciences, The University of New South Wales, Sydney, Australia

[e] Present address: UNSW RNA Institute, The University of New South Wales, Sydney, Australia

[f] Present address: Evolution & Ecology Research Centre, The University of New South Wales, Sydney, Australia

[g] Posgrado en Ciencias Biológicas, Universidad Nacional Autónoma de Mexico, CDMX, México

* Correspondence Laura Silva laura.silvar@cinvestav.mx

Abstract

Viruses are amongst the most prevalent pathogens that threaten plants. Plants have evolved a sequence-specific defense mechanism against viruses to ensure survival, known as RNA silencing, which includes transcriptional and post-transcriptional gene silencing. After a viral infection, some plants undergo recovery and become further resistant to viral infection. To identify additional mechanisms underlying disease recovery besides the known RNA silencing, we analyzed transgenic tobacco plants expressing a transcript derived from the Nuclear Inclusion "a" protein (NIa) cistron of the *tobacco etch virus* (TEV), which had recovered from infection three weeks following viral inoculation. Using *in situ* hybridizations and qRT-PCR, we detected the viral RNA and the transgene-derived transcript in stem sections adjacent to the recovered leaves. To further characterize the silenced and non-silenced conditions, we undertook tissue-specific RNA-Seq and small RNA-Seq analyses in leaf and stem. We found more differentially expressed genes (DEGs) in the recovered leaf, primarily related to defense, silencing, and hormone signaling responses. Finally, we observed differences in plasmodesmata callose deposition and callose-related genes. Overall, our findings suggest that cell-to-cell viral restriction movement also participates in the recovery of TEV infection in transgenic tobacco plants, besides the key function of RNA silencing.

Keywords: potyvirus; Tobacco etch virus (TEV); RNA silencing; plant-virus interaction; recovery; RNA-seq; callose deposition

1. Introduction

Viruses, together with fungi and bacteria, are among the most prevalent plant pathogens. Plants have developed specialized strategies to ensure survival in response to constant biotic and abiotic threats. Such strategies include innate and adaptive immune responses involving systemic acquired resistance (SAR) components and RNA interference (RNAi) machinery, respectively [1,2]. One of the possible outcomes of viral infection in plants is symptom recovery, characterized by the emergence of asymptomatic leaves at the apex after systemic symptomatic infection occurrence. Such recovered leaves are virus-free or present a reduction in virus titers and remain resistant to new inoculation of the same or highly related viruses. Recovery from viral disease was first documented in 1928 [1]; later, in 1993, it was linked to the RNA silencing machinery [2–4]. Recently, RNA silencing was shown to be the primary mechanism of viral recovering leaves [3]. Recovery occurs naturally in wild-type plants, especially those infected with positive-sense single-stranded (ss+) RNA viruses and DNA viruses like geminivirus, as well as in those transgenic plants expressing coding or non-coding sequences of the virus genome. Multiple studies have shown that infectious virus is not eliminated during the natural symptom recovery of wild-type plants induced by RNA viruses [5–7].

RNA silencing is a conserved sequence-specific defense mechanism against viruses that has been coopted as an endogenous gene regulatory mechanism. Silencing includes transcriptional (TGS) or post-transcriptional gene silencing (PTGS) [8,9]. PTGS results in the production of small RNAs with the participation of RNA-dependent RNA polymerases (RDRs) producing dsRNA, which are recognized and cleaved by Dicer-like 2 and 4 (DCL2, DCL4) [10,11]. These small dsRNAs can also arise from secondary RNA structures formed during viral genome replication. The resulting 21 to 24 nt cleavage small interfering RNAs

72 (siRNA) are then loaded onto Argonaute proteins AGO1 and AGO2, which form part of the
73 RNA-induced silencing complex (RISC). These AGO-associated siRNAs identify and enable
74 the cleavage of targets through sequence complementarity [12]. RDRs can further amplify
75 the RNA-silencing signal through the vascular system by synthesizing new dsRNA from
76 aberrant RISC-cleaved RNAs recruited by SGS3 [13,14]. Viruses have evolved proteins that
77 counteract silencing by siRNAs, known as VSRs (Viral Silencing Repressors), which
78 sequester virus-derived small RNAs and inhibit their incorporation into the RISC complex.
79 They can also interfere with the expression of the plant silencing machinery through the
80 inactivation or destabilization of RNAi and proteins or by promoting the expression of host
81 endogenous suppressors of RNA silencing (ESRs) such as Nbrgs-CaM (calmodulin from
82 *Nicotiana benthamiana* repressor of gene silencing). The RNAs of viruses encoding weak
83 VSRs, or transgenic plants producing low levels of transgene-derived transcripts, are
84 complemented with the virus-derived transcripts to surpass the RNA threshold level
85 necessary to trigger recovery [4,6,15].
86 Viral infection recovery mediated by RNA silencing has been primarily studied in leaves, as
87 this is the site where recovery is visually observed. Although much is known about the long-
88 distance movement of silencing signals across the stem, the role of this organ in phenomena
89 such as recovery remains poorly understood [16]. Here, we investigated the expression levels
90 of RNA silencing genes in the stem and leaf tissues during the final recovery stage after viral
91 infection. Additionally, to gain insights into the mechanisms underlying systemic recovery
92 in transgenic plants following viral infection, we looked for other genes that might be
93 differentially expressed between these two organs to identify additional mechanisms
94 underlying disease recovery besides the known RNA silencing observed in the leaves.
95

2. Materials and methods

2.1. Plant transformation

The viral NIa cistron sequence was initially cloned into the BamHI sites of plasmids pTL37/8595 containing both T7 and SP6 promoters [17]. Haploid leaf tissue of *Nicotiana tabacum* cultivars B49 and K326 plants was transformed via *Agrobacterium tumefaciens* [18]. A broad host range plasmid pPEV6 containing T-DNA borders, NIa gene, and the neomycin phosphotransferase II gene (that confers kanamycin resistance) selectable marker were mobilized from *E. coli* into *A. tumefaciens,* as described previously by Smith et al. (1994), and used to transform tobacco tissue. Transformed tissue was selected in the presence of 100 µg/mL of kanamycin sulfate. Doubled haploid plants were obtained from haploid mid-vein cultures [19]. These plants were allowed to seed, and the seeds were used for further studies. Burley 49 transformed plants are referred to as NIa.

2.2. Transgene expression

Transgenic seed screening was performed as described before [7]. To detect the transcript containing TEV NIa sequences, total leaf RNA was isolated using phenol:chloroform. Denaturing formaldehyde gels were blotted onto nylon membranes and hybridized with antisense 32P-labeled RNA probes. Such probes were obtained by an *in vitro* cell-free transcription system of plasmid pTL37/8595, containing the NIa gene insert, using SP6 RNA polymerase.

2.3. Nuclear run-off assays

Isolation of nuclei from non-transformed and transgenic plant tissue was performed according to [20], with a slight modification in the amount of starting tissue (we used 3 g of

120 leaves). DNA plasmids containing either the NIa insert, or the resident gene ubiquitin were
121 digested using HindIII restriction enzyme. Then, 5 μg of the restricted products were
122 electrophoresed in an agarose gel and blotted onto nylon membranes. Labelled 32P-RNA
123 transcripts for run-off reactions were added in equal amounts (estimated by specific counts
124 per million CPM) and used to hybridize the membranes containing DNA plasmids.
125
126 **2.4. Inoculation of transgenic plants and non-transformed plants**
127 In three independent replicates, 10 transgenic plants from each line were inoculated when
128 they reached approximately 30 cm tall. Plant leaves were lightly dusted with carborundum
129 and a 1:3 dilution of virus inoculum was applied with a cotton swab (dilution in w/v of virus-
130 infected plant tissue in deionized distilled sterile water). Plant viral symptoms were recorded
131 daily after the positive control plants started to show symptoms (8-10 days after inoculation).
132 Six recovered leaves from transgenic plants and six non-recovered leaves from WT plants
133 were inoculated with viral inoculum. This procedure was performed twice and surveyed for
134 symptoms.
135 For the inoculation of wild type plants using transgenic stem or leaf tissues of recovered
136 plants, we used the same dilution as before in six replicates and the experiment was repeated
137 twice.
138
139
140 **2.5 *In situ* hybridization**
141 *In situ* hybridization was performed as described [21] with modifications. For synthesizing
142 sense and anti-sense 11-digoxigenin-UTP labelled probes, a pTC plasmid containing a 1290-
143 bp NIa fragment was linearized with restriction enzymes PsT I, and 1 μg was used as a probe

144 synthesis template. RNA probes were synthesized using DIG northern starter kit (Roche,
145 Mannheim, Germany). Transgenic non-inoculated (NIa-N plants) or TEV-inoculated and in
146 process of recovery (NIa-PR1-PR3 and R) were fixed as described by [22]. RNA probes were
147 hydrolyzed following the method described by [21], and 3%–6% of each labelling reaction
148 (100–400 ng of RNA) was mixed with 40 µL of 50% formamide, added to 200 µL of
149 hybridization buffer, and used as a probe for a pair of slides. Overnight hybridization was
150 performed as described by [22].
151
152 **2.6. Northern hybridization**
153 Total RNA was resolved on a denaturing 0.8% agarose gel. Gels were transferred to a
154 HybondN+ membrane (Amersham, Piscataway, NJ, USA). Hybridizations were performed
155 with viral-derived probes labelled with a dCTP^{32}P.
156
157 **2.7. RNA extraction and Illumina Sequencing**
158 Total RNA extraction was performed as described by [23]. Briefly, tissue was collected from
159 leaves or stems from 4 plants in the process of recovery of PR3 and grounded in liquid
160 nitrogen. A total of 4 RNA-Seq libraries (2 tissues, 2 replicates per tissue 2x100) were
161 prepared and sequenced at Labsergen facilities (Irapuato, Mexico) using Illumina HiSeq2500
162 (Hayward, CA, USA). Raw data is publicly available at NCBI, BioProject accession:
163 PRJNA844420.
164
165 **2.8. Mapping and statistical analysis**
166 Trimming and cleaning of reads were conducted according to [24]. Cleaned and trimmed
167 reads were aligned against the reference tobacco transcriptome Nitab-v4.5

168 (www.solgenomics.net) [25,26] to quantify the expression of all transcripts using Kallisto v
169 v0.46.2. Kallisto was executed with bias correction and 1000 bootstrap. Differential
170 expression analysis was conducted with Sleuth v0.30.0 [27]. Reads of each library were
171 mapped with a percentage of 81.05% pseudoaligned and 80.75% pseudoaligned just once to
172 the transcriptome (Table S1). After the differential expression analysis, transcripts with log2
173 FoldChange (log2FC) values of ≥1 and ≤-1 and q-value of ≤0.05 were considered as
174 differentially expressed genes (DEGs).
175

176 **2.9. Functional annotation and gene expression validation**

177 To identify the Gene Ontology enrichment, Singular Enrichment Analysis (SEA) was
178 performed with AgriGO v2 with the Nitab4.5 (www.solgenomics.net) background under
179 Fisher and the multi-test adjustment method of Hochberg (FDR) with a p-value ≤0.05 [28].
180 Ontology reduction and network construction were performed with REVIGO with standard
181 parameters (medium 0.7 resulting list) and Cytoscape v3.8.0 [29,30]. Validation of gene
182 expression and the presence of CP (viral) and NIa (viral and/or transgene) RNAs in leaves or
183 stems was performed using quantitative reverse transcription PCR (qRT-PCR). The
184 experiments were conducted on a StepOne Real-Time PCR System (Applied Biosystems)
185 with qPCR SybrMaster HighROX (Jena Bioscience, Germany). The qRT-PCR was carried
186 out under a three-step PCR protocol, with an alignment step at 60°C for 30 seconds.
187 The relative quantification of gene expression was determined using the double delta Ct (2^{-}
188 $^{\Delta\Delta Ct}$) method, with actin serving as the housekeeping gene for normalization. The specific
189 primers used for amplifying the different genes are listed in Table S2.
190

191 **2.10. Small RNA analysis**

192 A total of 4 small RNA-Seq libraries (2 treatments, 2 replicates per treatment 1x36) were
193 prepared with gel band selection and sequenced at Cinvestav facilities (Irapuato, Mexico)
194 using the Illumina HiSeq2500 (Hayward, CA, USA) platform. Raw data are publicly
195 available at NCBI, BioProject accession: PRJNA844411. Reads were mapped with Bowtie
196 v1.2.3 (--best --strata parameters) to the tobacco and TEV concatenated genomes, then
197 miRNA prediction was carried out with ShortStack v3.8.5 standard parameters only
198 quantifying miRNAs annotated in the miRBase database [31]. Differential expression
199 analysis was carried out with DeSeq2 v1.36.0 standard parameters, and the target prediction
200 of differentially expressed miRNA was carried out using psRNATarget 2017 V2 schema
201 standard parameters [32].
202
203 **2.11. Callose deposition analyzed by aniline blue multiphoton microscopy**
204 Sections of 3 leaves and stems of NIa-plants at the PR3 and mock3 stage, and WT I3 and
205 mock3 were cut and fixed in 4% formaldehyde, faded with 96% alcohol, and processed after
206 the addition of SynaptoRed C2 as stated by the manufacturer (Biotium, Fremont, CA, USA),
207 aniline blue staining was carried out following the methodology described by [33].
208 Multiphoton images were taken with an LSM 880-NLO Axio Imager Z2 microscope (Zeiss,
209 Germany) coupled to a Ti:Sapphire infrared laser (Chameleon Vision II, COHERENT,
210 Scotland). The laser wavelength was set at 723 nm for aniline blue and 800 nm for
211 SynaptoRedC2, both dyes were detected at a 300-685 nm wavelength window with a Non-
212 Descanned Detection.2 (NDD.2) using a 500-550 nm filter (Zeiss, Germany). Callose
213 quantification was performed as described by [33].
214
215 **3. Results**

216 **3.1. NIa-transgene expression and recovery**

217 Following TEV infection, transgenic tobacco plants expressing either an untranslatable or a
218 translatable version of the TEV NIa cistron (Figure S1) developed a systemic infection
219 characterized by mosaic symptoms in the inoculated leaf and the three leaves immediately
220 above the inoculated one (Figure 1). The process of recovery (PR) assessed as a symptom
221 reduction was first observed in the interveinal regions of the leaf above the inoculated one
222 (Nla-PR1) as well-defined chlorotic areas or speckles in interveinal regions. Between 14 to
223 21 days post-inoculation (dpi), the PR progressively increased in leaves 2 (NIa-PR2) and 3
224 (NIa-PR3), *i.e.,* NIa-PR1< NIa-PR2< NIa-PR3, registering an almost complete recovered
225 leaf 4 (NIa-R4) (Figure 1a) sometimes with a reduced chlorotic speckle at the tip of the leaf.
226 Once recovered, the leaves remained highly resistant to the virus as they showed no viral
227 symptoms compared to WT plants. In contrast, all the leaves of WT plants remained
228 symptomatic, showing chlorosis, while those of mock-inoculated NIa tobacco (NIa-N1-4)
229 developed normally (Figure 1b and c, respectively). As expected, no infection was observed
230 when fully recovered leaves were used as a source of inoculum in healthy plants (Figure S2).

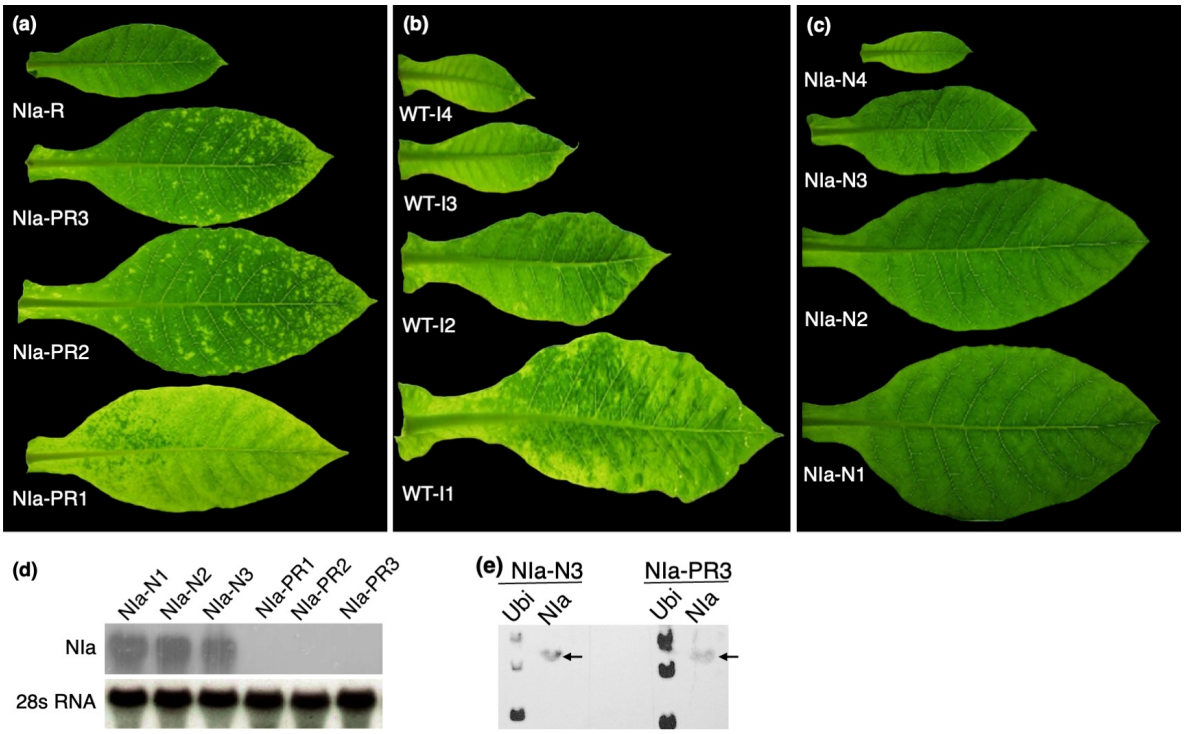

Figure 1: RNA silencing is involved in progressively recovering leaves from NIa plants. **(a)** Inoculated NIa plants in the process of recovery (NIa-PR1-3) and fully recovered (NIa-R) **(b)** Inoculated B49 wild-type plants (WT-I1-4). **(c)** The representative phenotype of mock-inoculated NIa plants (NIa-N1-4). **(d)** Northern blot of the NIa viral transgene-derived transcripts and 28S RNA (mostly cytoplasmic) of NIa-N1-3 and NIa-PR1-3 leaf tissue. **(e)** Run-off assay of the endogenous plant ubiquitin and viral transgene-derived transcripts in the extracted nucleus in leaves of NIa-PR3 and NIa-N3.

3.2 PTGS is involved in transgenic NIa-tobacco recovery

We confirmed that the PR observed in the leaves of NIa plants resulted from PTGS. By Northern blot, the expected band corresponding to the NIa RNA transcript is detected in NIa-N1-3 but not in NIa-PR1-3 leaves (Figure 1d). However, nuclear transcription rates of the transgene-derived NIa cistron and the endogenous ubiquitin gene were similar in mock-

246 inoculated and recovered tissue at a similar physiological stage (NIa-N3 and NIa-PR3 at 21
247 dpi, integrated density values, IDV = 1.99 and 2.20, respectively). The multiple bands in the
248 ubiquitin control lane resulted from incomplete digestion of the plasmid blotted onto the
249 membrane (Figure 1e). This indicated that NIa transgene expression is similar in both the
250 nuclei of plants in the process of recovery and mock-inoculated plants, and that recovery and
251 viral gene silencing were activated following virus replication in the cytoplasm. The presence
252 of the viral transgene-derived transcript in the nucleus and its absence in the cytoplasm
253 suggested that PTGS was active during the recovery process.
254

255 **3.3 Stem and leaf-vascular tissue did not undergo silencing as shown by *in situ***
256 **hybridization**

257 We used the antisense viral NIa segment as an RNA probe to detect viral and/or transgene-
258 derived transcripts in the leaf blade and leaf stem base, *i.e.,* the area of the stem that connects
259 to the petiole, of NIa-N and NIa-PR plants by *in situ* hybridization (Figure 2). A positive
260 signal in NIa-N tissues indicated the presence of the transgene-derived transcript. In contrast,
261 the corresponding signal in NIa-PR tissues indicated the presence of viral transcript due to
262 infection or the transgene-derived transcript. In the leaf blade, we observed transgene-derived
263 transcript in NIa-N1-3 leaves (Figure 2a), whereas very faint or no signal was detected in
264 NIa-PR leaves (Figure c). This observation indicated RNA silencing of both the viral-derived
265 transcript and the virus. Conversely, viral and/or transgene expression at the stem was
266 observed in both mock and viral inoculated NIa plants (Figure 2b and d). In mock plants, we
267 observed a strong transcript signal in all cell types, including upper and lower epidermis,
268 palisade, and spongy parenchyma, with higher intensity in the nucleus. Vascular bundles also
269 presented a strong transcript signal. In the stem, phloem cells (companion cells and sieve

elements) showed evidence of the transgene-derived transcript (Figure 2a-b). In some areas, phloem parenchyma cells were also indicative of the presence of the transcript. The brown color is due to non-specific background signal.

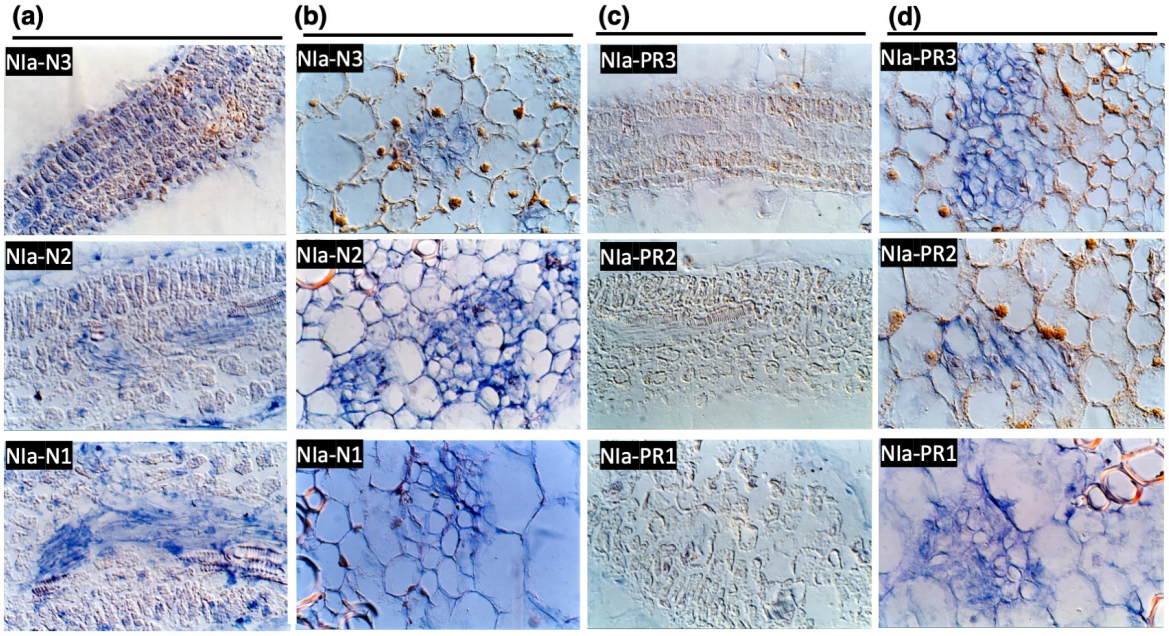

Figure 2: RNA silencing occurred in leaves but not in stems of infected NIa plants. The presence or absence of TEV-NIa RNA derived from the transgene and/or viral transcript was analyzed by *in situ* hybridization. **(a)** Leaves and **(b)** stems of transgenic mock-infected plants (NIa-N1-3). **(c)** Leaves in the process of recovery of transgenic infected plants (NIa-PR1-3) and **(d)** the corresponding sections of their stems.

Stem and leaves cut sections of NIa-PR3 were used as the source of inoculum in healthy WT plants; those inoculated with NIa-PR3 leaves remained symptomless. Meanwhile, plants inoculated with NIa-PR3 stems developed a symptomatic TEV infection (Figure S2). Furthermore, qRT-PCR carried out on CP RNA (viral) and NIa (viral and/or transgene) did not amplify the CP on NIa-PR3 leaves (Figure S3). These results validate the *in-situ*

hybridization observation of absence of TEV in leaves and its presence and/or the NIa derived transcript in stems.

As expected, mock-inoculated WT B49 plants showed no evidence of viral expression in the leaf or stem. In contrast, the inoculated counterparts showed hybridization profiles like mock-inoculated NIa plants, albeit with a slight reduction of virus signal in leaves 2 and 3 (Figure S4).

The boundary zone at the stem-petiole insertion presented a differential accumulation of signal derived from the viral transcript of NIa (Figure 3). For instance, NIa RNA accumulated in the stem rather than in the petiole, except for the petiole vasculature, where NIa RNA was present (Figure 3a). Likewise, NIa was present in the leaf vasculature but not in the mesophyll tissue when we analyzed longitudinal sections of the leaf (Figure 3b).

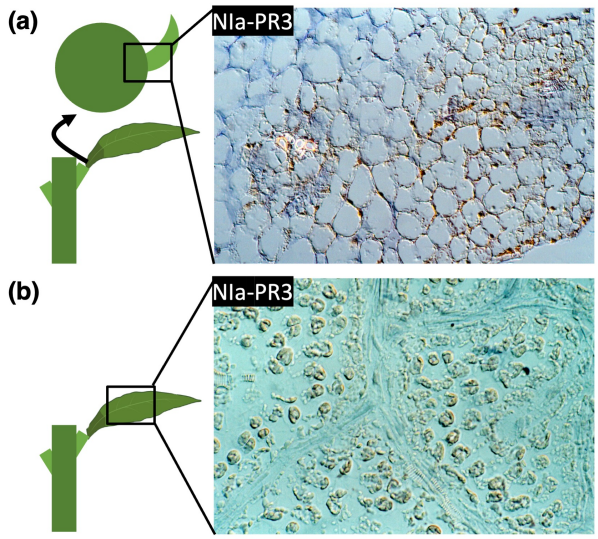

Figure 3: Vicinity between silenced leaf with non-silenced vasculature and non-silenced stem. *In situ* hybridization of RNA of tobacco TEV-NIa plants at the: **(a)** junction of stem-petiole insertion of NIa-PR3 plant and **(b)** leaf section of an NIa-PR3 plant showing non-silenced vasculature and silenced mesophyll cells.

302 **3.4. Defense-related genes were overexpressed in leaf**

303 To explore leaf and stem-specific responses to TEV during recovery, we performed high
304 throughput RNA sequencing using transgenic NIa-plants at the PR3 stage. We identified 731
305 differentially expressed genes (DEGs) (log2FC ≥1 and ≤-1 and q-value of ≤0.05); among
306 them, 700 DEGs corresponded to the leaf and 31 DEGs to the stem. The identified DEGs
307 were enriched for functions related to the "binding" molecular function (MF) in the stem. On
308 the other hand, 16 enriched biological processes (BP) were identified in the leaf, including
309 "defense response", "regulation of RNA metabolism", "protein phosphorylation", and
310 "ubiquitination" (Fig. S5). Similarly, 17 MFs including "oxidoreductase activity", "protein
311 binding", "sequence-specific DNA binding", and "transcription factor activity" were
312 enriched in this tissue. Overall, we found 28 disease-resistance, 8 jasmonic acid, and 3
313 ethylene-related genes differentially expressed in the leaf (Table S3), whereas no defense-
314 related genes were differentially expressed in the stem.

315

316 **3.5. The silencing machinery was overexpressed in the leaf, while suppressors of**
317 **silencing were overexpressed in the stem**

318 As silencing has been reported as the principal mechanism of recovery, we analyzed nine key
319 silencing genes (DCL2, DCL4, SGS3, HEN1, NRPD1a, RDR6, RDR2, AGO1, and AGO2)
320 differentially expressed. We found that four of the nine key RNA silencing genes, namely
321 AGO1, DCL2, HEN1, and RDR6, were overexpressed in the leaf compared to the stem
322 (Table 1). The other five genes were not differentially expressed. Moreover, in the stem, we
323 found one transcript encoding for the calmodulin-binding protein-like (rgs-CML), a virus-
324 triggered endogenous suppressor of RNA silencing well-characterized in tobacco (Table 1).

325

Table 1. Silencing and repressor of gene silencing related DEGs expressed at leaf or stem.

Gene	Log2FC	Tissue
Calmodulin binding protein-like (rgs-CML)	1.58	Stem
Argonaute 1 (AGO1)	1.62	Leaf
Dicer-like 2 (DCL2)	1.95	Leaf
Hua enhancer 1 (HEN1)	1.5	Leaf
RNA-dependent RNA polymerase (RDR6)	2.43	Leaf

326

327 **3.6. Callose accumulation in the leaf suggested restriction of viral cell-to-cell**

328 **movement by plasmodesmata**

329 We further analyzed differences in the expression patterns of genes involved in viral

330 movement across tissues. Notably, for the leaves we found we found overexpression of genes

331 encoding for enzymes related to callose synthesis (three glucan synthase-like enzymes -GSL,

332 and one callose synthase -CALS), and five genes related to callose accumulation at

333 plasmodesmata (Table 2). The expression levels of rgs-CML, DCL2, AGO1, RDR6, GSL12

334 and CALS1 were validated by qRT-PCR (Figure S6).

Table 2. Callose synthase and deposition at plasmodesmata DEGs expressed in the leaf.

Gene	Log2FC
GLUCAN SYNTHASE-LIKE 12 (GSL12)	4.58
CALLOSE SYNTHASE 1 (CALS1)	2.85
CADMIUM SENSITIVE 1 (CAD1)	2.08
GLUCAN SYNTHASE-LIKE 1 (GSL1)	1.99
IRREGULAR XYLEM 1 (IRX1)	1.43
PENETRATION 3 (PEN3)	1.42
GLUCAN SYNTHASE-LIKE 3 (GSL03)	1.2
UDP-GLUCOSYL TRANSFERASE 74B1 (UGT74B1)	1.17
CELLULOSE SYNTHASE A4 (CESA4)	1.11

335

336 Following these results, we decided to stain NIa-PR3, NIa-mock3, WT-I3 and WT-mock3
337 leaves and stems with aniline blue to corroborate callose deposition at NIa-PR3 leaf
338 plasmodesmata. In NIa-PR3 leaves, we found a significantly enhanced callose deposition
339 compared to NIa-mock3, and callose accumulation was higher in NIa-PR3 leaves than WT
340 mock or infected leaves (Figure 4a-b). In NIa-PR3 stems, callose accumulation was reduced
341 in comparison with the other samples. However, this difference was not significant. We
342 found a significant reduction of callose accumulation in infected leaves of WT plants, but no
343 difference was shown between the infected and mock stems (Figure 4). These results
344 corroborate the overexpression of callose accumulation-related genes at NIa-PR3 leaves.

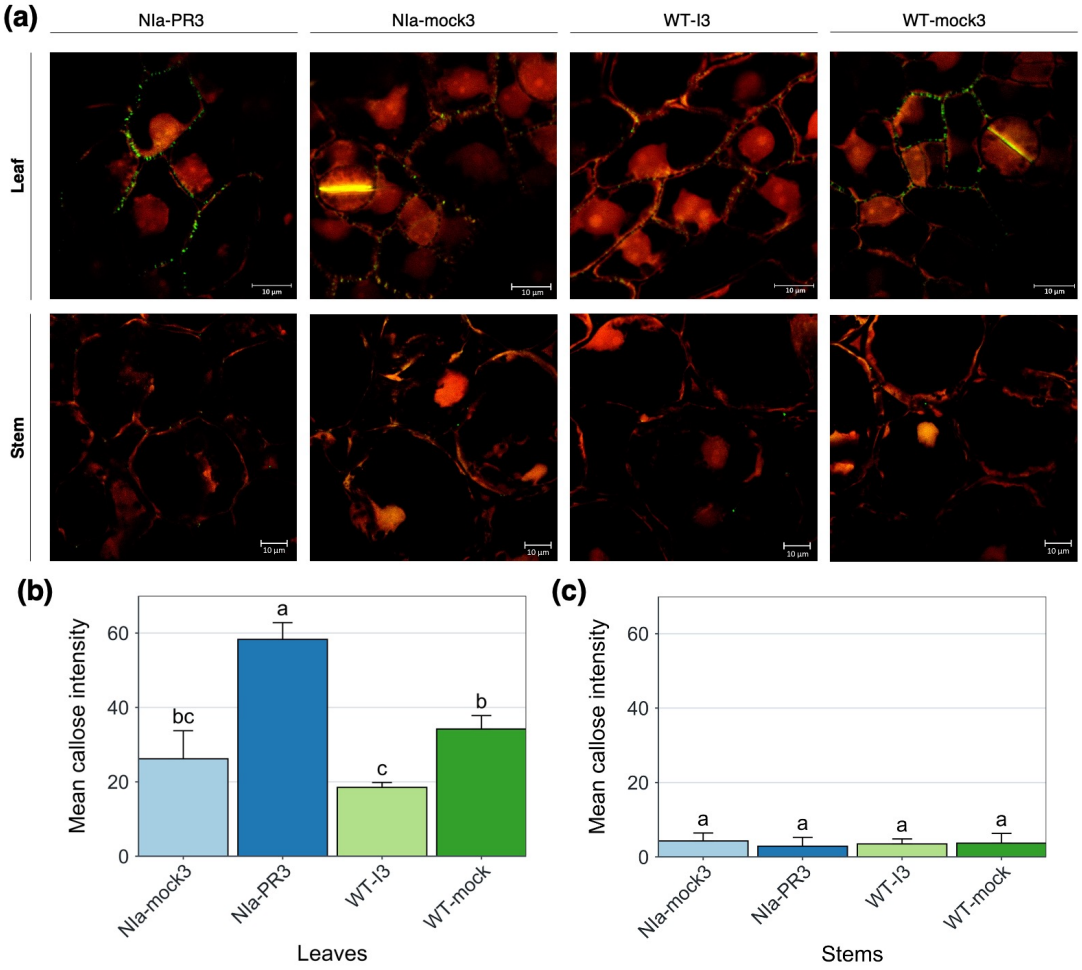

345

346 Figure 4: Plasmodesmata callose deposition in leaves and stems of NIa and WT plants. **(a)**
347 Differences in callose deposition were observed using multiphoton imaging of aniline blue
348 fluorescence. The red stain in the images corresponds to SynaptoRedC2 (plasma membrane
349 staining), and the green color corresponds to aniline blue dye (callose staining). (b)
350 Quantification of leaves callose deposits at plasmodesmata as observed after microscopy. (c)
351 Quantification of stems callose deposits at plasmodesmata as observed after microscopy.
352 Letters show grouping p-value <= 0.05 Tukey's test.
353

354 **3.7. Plant miRNA and vsiRNA profiles**

355 A total of 12 miRNA were detected to be differentially expressed (p-value ≤0.05) in the leaf
356 and 4 in the stem, with 77 and 6 predicted targets, respectively. Functional enrichment
357 analysis of leaf miRNAs targets showed a negative regulation of macromolecule
358 modification, protein phosphorylation, response to stimulus, response to stress, defense
359 response and gene silencing by RNA (Fig. 5a) with miRNA targets of plant-pathogen
360 interaction pathway and disease resistance (Table S4). Meanwhile, enrichment for stem
361 miRNA did not show any functional enrichment.
362 Virus-derived small interfering RNAs (vsiRNAs) are commonly produced during viral
363 infections and work as keystone molecules for effective viral silencing. In this study, we
364 observed that vsiRNA was more abundant in the stem than in leaves (489.89 CPMx10^{-3} and
365 448.96 CPMx10^{-3}, respectively). However, 24 nt vsiRNAs were more abundant in the leaf,
366 which could suggest a role for DCL3 in their biogenesis. Surprisingly, we did not observe
367 differential expression of DCL3 in the leaf (Fig. 5b, Table 1). TEV genome-wide
368 accumulation of vsiRNAs revealed *per-site* differences, with higher abundance at the P1
369 cistron than other genomic regions, including the NIa transgene (Fig. 5c). Log2Fold change

370 was calculated to compare vsiRNA genome accumulation between leaf and stem. We found
371 an overall lower vsiRNA accumulation in the leaf (Figure S7). In addition, we found
372 remarkable differences in the negative-stranded vsiRNA of P3 and CI cistrons between leaf
373 and stem, suggesting these RNAs could be important in maintaining a non-silenced stem
374 (Figure S7b).
375 It has been proposed that vsiRNA has the potential to regulate host gene expression [34]
376 Therefore, we investigated if vsiRNA derived from the top 20 abundant sites and P3 and CI
377 cistrons target plant host genes. The resulting predicted target genes in the tobacco of both
378 abundant and non-abundant vsiRNAs were not functionally enriched. However, we found
379 that the stem-derived-vsiRNA arising from the P3 cistron region between ~3200-3300nt (-)
380 targets GSL03, a tobacco gene involved in viral movement restriction. Also, the most
381 abundant vsiRNAs derived from the P1 and HC-Pro (~900nt and ~1600nt) region are
382 predicted to target both DCL4 and PR1. No defense-related target genes were found in the
383 non-abundant regions.
384

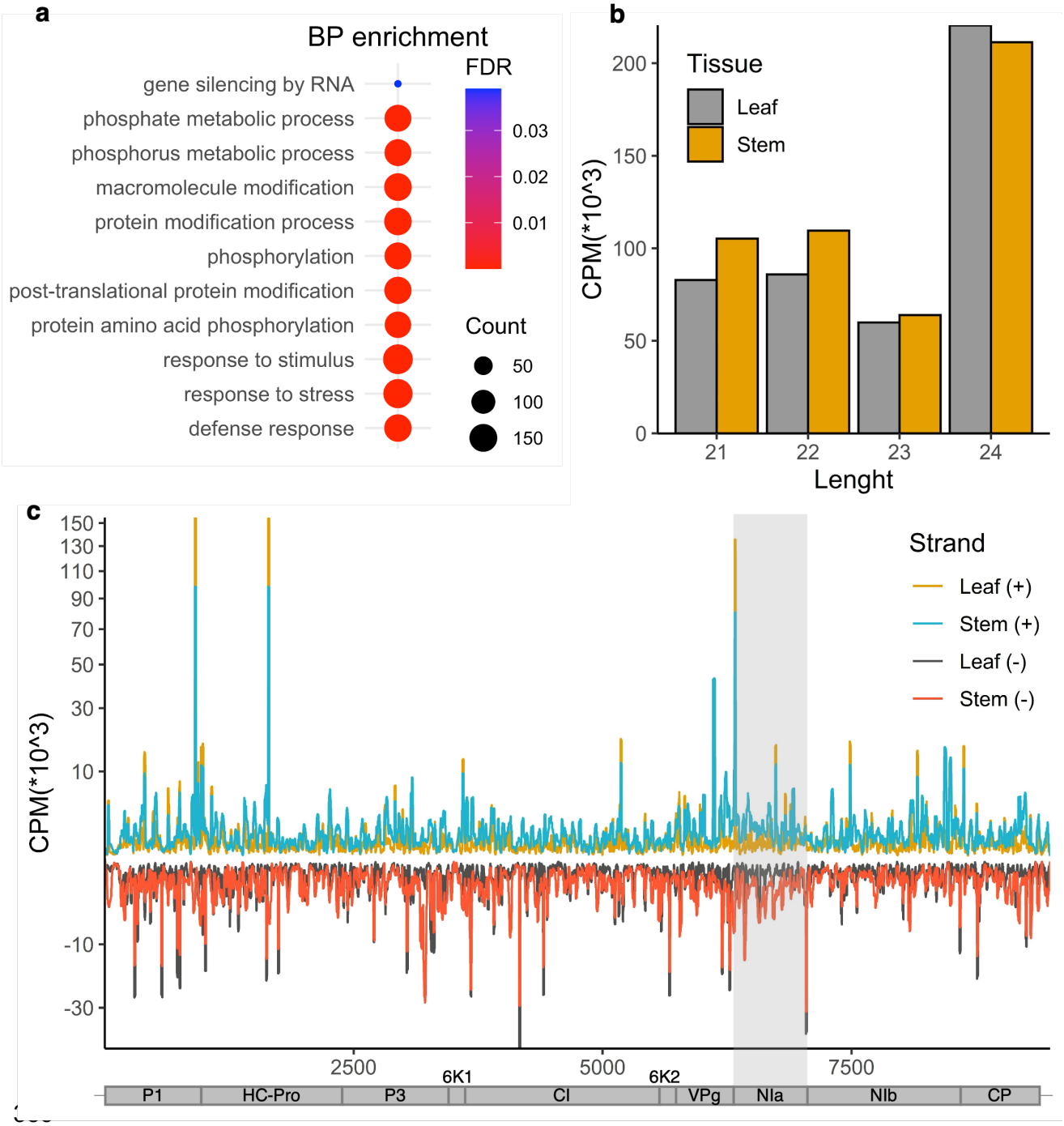

Figure 5: Plant miRNA and vsiRNA profiles in leaves and stem of NIa-PR3 plants. **(a)** Functional enrichment network of Leaf miRNAs. **(b)** Per tissue abundance of 21, 22, 23, and 24 nt vsiRNA. **(c)** TEV genome-wide distribution of vsiRNA in counts per million (CPM).

390 **4. Discussion**

391 **4.1. Plants undergo a process of recovery which is compartmentalized**

392 We suggest that the process of recovery in leaves of NIa plants resulted from PTGS, as in
393 other recovery systems [3]. Recovered tissues remain resistant to the virus, as reported before
394 in other transgenic tobacco plants expressing the TEV-viral coat protein cistron [17]. The
395 presence of the virus in the stem and leaf vasculature but not in the mesophilic cells suggested
396 restriction of intracellular movement of TEV, possibly occurring at the exit from the phloem.
397 Previous studies have shown that not all the new emerging organs are fully recovered, as we
398 saw between the recovered leaves and non-recovered stems in the present study. However,
399 none of these works compared the differences between recovered and non-recovered tissues
400 [35,36].

401

402 **4.2. RNA silencing and viral movement restriction at leaf and stem**

403 It is well known that RNA silencing plays a key role in recovery, as the elimination of
404 components of the RNA silencing machinery halts plant recovery [35,37]. Viruses that
405 efficiently counteract RNA silencing evade recovery [38,39]. Here we found that genes that
406 are essential for RNA silencing, including AGO1, DCL2, HEN1, and RDR6, were
407 overexpressed in the leaf but not in the stem. Interestingly, AGO2 was not differentially
408 expressed, albeit previously described as the main silencing gene involved in antiviral
409 defense [12]. Similarly, other key genes for VIGS and siRNA biogenesis, such as SGS3 and
410 SDE5, and key genes related to PTGS-TGS crosstalk, such as NRPD and RDR2, were not
411 differentially expressed in the stem [37,40,41]. These findings suggest that other factors may
412 be involved in the stem repression of silencing since some key silencing-related genes are
413 equally expressed in both tissues (DCL3-4, SGS3, NRPD1a, RDR2, and AGO2). In this

414 regard, we found that the plant endogenous rgsCaM was overexpressed in the stem,
415 suggesting it may participate in silencing suppression, as it is known to be recruited by TEV
416 HC-Pro to suppress RNA silencing [42] and may explain the lower expression of RDR6 [43].
417 Moreover, rgsCaM is also known to enhance virus resistance by targeting itself and HC-Pro
418 to proteolytic pathways, thus restricting viral infections to local areas [44]. In this sense, the
419 overexpression of rgsCaM could explain the lack of silencing in the stem and enhancement
420 of antiviral responses restricting viral infection to this tissue.
421
422 Another point to consider is that RNAi components could be transported from the leaves to
423 the stem based on local RNA expression levels. While RNA silencing genes were not
424 overexpressed in the stem, this does not necessarily mean their proteins or RNAi products
425 are inactive in this tissue. It is plausible that RNAi elements, such as siRNAs or silencing-
426 associated proteins, are shuttled from the leaves to the stem, contributing to antiviral defense.
427 Further studies are needed to determine whether RNAi components generated in the leaves
428 are transported to the stem and how they function in regulating viral silencing and movement
429 across tissues [45–47].
430
431 **4.3. Plant innate immunity also participates in plant recovery**
432 The lack of tissue recovery in tissues such as the meristem has been attributed to RNA
433 silencing and is considered a key step in viral recovery [48]. Recent works provide evidence
434 that silencing is not the reason for tissue exclusion of recovery, as DCL2/4-silenced plants
435 infected with CymRSV were free of the virus at the meristem [49]. Most of the literature
436 describes recovery by specific components in the RNA silencing pathway rather than
437 considering the global changes occurring in a plant during the recovery process. PAMP-

438 triggered immunity (PTI) has been reported to be prevalent in almost all plant-virus
439 transcriptomes. Indeed, we detected many genes involved in PTI and canonical defense
440 overexpressed in the leaf. For instance, nine genes related to callose deposition at
441 plasmodesmata or negative regulators of plasmodesmata permeability (GSL12, GSL1,
442 GSL03, CALS1, CAD1, IRX1, PEN3, UGT74B1, and CESA4) were overexpressed in the
443 leaf. In agreement with these observations, we corroborated callose accumulation by image
444 microscopy in the leaf. Similar to our findings, a Cassava line resistant to CBSV allowed
445 viral transmission through the stem, whereas no virus could be detected in leaves [50]. In the
446 following study, the authors found overexpression of b-1,3-GLUCANASE, ANKs, and
447 PDLP1 genes in the susceptible line. These genes participated in plasmodesmata
448 permeability as the viral movement-promoting factors, whereas GSL4 (a possible negative
449 regulator of plasmodesmata permeability) was overexpressed in both susceptible and
450 resistant lines [51]. However, we did not find any viral movement promotor overexpressed
451 in the stem, which suggests that, in our system, viral movement restriction is exerted through
452 a pathway different to the one identified in CBSV-resistant Cassava.
453
454 **4.4. vsiRNA accumulation at leaf and stem**
455 Contrary to the findings in ORMV-infected Arabidopsis plants, which had a high amount of
456 21-22nt vsiRNA accumulated in recovered actively virus-infected leaves [37], in this study,
457 we quantified around 20% less 21-23nt vsiRNAs in recovered tissue (leaf) than in non-
458 recovered stem. Out of the 7 genes dubbed crucial for recovery [37,41] four (AGO1, DCL2,
459 HEN1, and RDR6) were overexpressed in the leaf compared with the stem. The higher
460 accumulation of vsiRNAs at the stem could be explained by an active replication of the virus
461 in this tissue. Despite the overexpression of DCL2 (involved in 22nt production) in leaves,

462 we found more accumulation of 24nt than 21-23nt vsiRNAs. Because it is more common that
463 21-22nt vsiRNAs accumulate in higher amounts than 23-24nt vsiRNAs during viral
464 infections [52,53], further investigation needs to be performed to explain our differential
465 findings. We observed a higher accumulation of positive-strand vsiRNAs, which has been
466 previously found to be common in positive-stranded RNA viruses [52]. The non-random
467 distribution of vsiRNAs along the TEV genome is also common and is associated with the
468 fold-back structures of the genomic RNA and binding of the vsiRNAs to the viral HC-Pro
469 [54–56]. vsiRNA accumulation hotspots have been previously associated with the
470 modulation of pathogenesis in the host machinery by alphavirus-derived small RNAs, which
471 influence infection outcomes in disease vector mosquitoes [34]. However, in our work no
472 vsiRNAs arising from any of the top 20 accumulation hotspots had predicted target genes
473 involved in defense or the pathogenesis response in the host, including those arising from
474 differential hotspots between leaves and the stem. But vsiRNAs do target GSL03 gene
475 involved in viral movement restriction
476

477 **5. Conclusions**

478 Here we show that additional host mechanisms, such as the overexpression of defense-related
479 genes and callose accumulation at plasmodesmata, contribute to viral disease recovery,
480 complementing RNA silencing. We also bring insights that compartmentalization of RNA
481 (viral of transgene derived) or specialization of recovery differentially occurs between leaves
482 and stems since RNA silencing and plant defense responses are mounted differently in such
483 tissues. It is also possible that RNAi components produced in the leaves may be transported
484 to the stem, where they still contribute to antiviral defense, highlighting the importance of
485 both local and systemic RNA silencing activity. Thus, this study opens the window to

486 investigate whether defense responses innate and adaptive to viruses or other pathogens are
487 also differentially triggered in other plant organs. Understanding this compartmentalization
488 would allow the designing of new strategies to control diseases.
489
490 **Declaration of competing interest**
491 The authors declare no conflict of interest.
492
493 **Data availability**
494 The raw reads generated during the current study are publicly available at NCBI under
495 PRJNA844420, PRJNA844411 accession numbers. Materials are available from the
496 corresponding author upon reasonable request.
497
498 **Acknowledgments**
499 We thank Gabriela Chávez-Calvillo, Gustavo Rodríguez-Gómez, Domitila J. Rosales, Dalia
500 Rodríguez-Ríos, José N. Santoyo-Villa and Luis J. Saucedo-Vargas and PlanTecc for their
501 technical support. This research was supported by grants from Cinvestav (IP 1995) and
502 CONACyT (4274-N9406). LSR and SLFV supervised the study. LSR, PVM, and AOL
503 designed the experiments. PVM, AOL and CMFG performed the experiments. PVM
504 analyzed the data and wrote the manuscript. LSR, SLFV, GL and PVM edited the manuscript.
505 JPVC directed the in-situ hybridization work performed in 2000. All authors read and
506 approved the final manuscript. This paper is part of the productivity of the Doctoral degree
507 of P.V.M. at the Posgrado en Ciencias Biológicas, UNAM.
508
509

510 **References**

511 [1] S.A. Wingard, Hosts and symptoms of ring spot, a virus disease of plants, J. Agric.
512 Res. 37 (1928) 127–153.
513 [2] L. Bengyella, S.D. Waikhom, F. Allie, C. Rey, Virus tolerance and recovery from viral
514 induced-symptoms in plants are associated with transcriptome reprograming, Plant
515 Mol Biol 89 (2015) 243–252. https://doi.org/10.1007/s11103-015-0362-6.
516 [3] B. Ghoshal, H. Sanfaçon, Symptom recovery in virus-infected plants: Revisiting the
517 role of RNA silencing mechanisms, Virology 479–480 (2015) 167–179.
518 https://doi.org/10.1016/j.virol.2015.01.008.
519 [4] J.A. Lindbo, L. Silva-Rosales, W.M. Proebsting, W.G. Dougherty, Induction of a
520 Highly Specific Antiviral State in Transgenic Plants: Implications for Regulation of
521 Gene Expression and Virus Resistance., The Plant Cell 5 (1993) 1749–1759.
522 https://doi.org/10.1105/tpc.5.12.1749.
523 [5] M. Aregger, B.K. Borah, J. Seguin, R. Rajeswaran, E.G. Gubaeva, A.S. Zvereva, D.
524 Windels, F. Vazquez, T. Blevins, L. Farinelli, M.M. Pooggin, Primary and secondary
525 siRNAs in geminivirus-induced gene silencing, PLoS Pathog. 8 (2012) e1002941.
526 https://doi.org/10.1371/journal.ppat.1002941.
527 [6] E. Santovito, T. Mascia, S.A. Siddiqui, S.A. Minutillo, J.P.T. Valkonen, D. Gallitelli,
528 Infection Cycle of Artichoke Italian Latent Virus in Tobacco Plants: Meristem Invasion
529 and Recovery from Disease Symptoms, PLOS ONE 9 (2014) e99446.
530 https://doi.org/10.1371/journal.pone.0099446.
531 [7] L. Silva-Rosales, J.A. Lindbo, W.G. Dougherty, Analysis of transgenic tobacco plants
532 expressing a truncated form of a potyvirus coat protein nucleotide sequence, Plant
533 Mol. Biol. 24 (1994) 929–939. https://doi.org/10.1007/bf00014446.
534 [8] S.-W. Ding, O. Voinnet, Antiviral Immunity Directed by Small RNAs, Cell 130 (2007)
535 413–426. https://doi.org/10.1016/j.cell.2007.07.039.
536 [9] X.-B. Wang, J. Jovel, P. Udomporn, Y. Wang, Q. Wu, W.-X. Li, V. Gasciolli, H.
537 Vaucheret, S.-W. Ding, The 21-Nucleotide, but Not 22-Nucleotide, Viral Secondary
538 Small Interfering RNAs Direct Potent Antiviral Defense by Two Cooperative
539 Argonautes in Arabidopsis thaliana, The Plant Cell 23 (2011) 1625–1638.
540 https://doi.org/10.1105/tpc.110.082305.
541 [10] A. Niehl, I. Wyrsch, T. Boller, M. Heinlein, Double-stranded RNAs induce a pattern-
542 triggered immune signaling pathway in plants, New Phytologist 211 (2016) 1008–
543 1019. https://doi.org/10.1111/nph.13944.
544 [11] N. Pumplin, O. Voinnet, RNA silencing suppression by plant pathogens: defence,
545 counter-defence and counter-counter-defence, Nat Rev Microbiol 11 (2013) 745–760.
546 https://doi.org/10.1038/nrmicro3120.
547 [12] M. Jaubert, S. Bhattacharjee, A.F.S. Mello, K.L. Perry, P. Moffett, ARGONAUTE2
548 mediates RNA-silencing antiviral defenses against Potato virus X in Arabidopsis,
549 Plant Physiol. 156 (2011) 1556–1564. https://doi.org/10.1104/pp.111.178012.
550 [13] N. Kumakura, A. Takeda, Y. Fujioka, H. Motose, R. Takano, Y. Watanabe, SGS3 and
551 RDR6 interact and colocalize in cytoplasmic SGS3/RDR6-bodies, FEBS Letters 583
552 (2009) 1261–1266. https://doi.org/10.1016/j.febslet.2009.03.055.
553 [14] A. Peragine, M. Yoshikawa, G. Wu, H.L. Albrecht, R.S. Poethig, SGS3 and
554 SGS2/SDE1/RDR6 are required for juvenile development and the production of trans-
555 acting siRNAs in Arabidopsis, Genes Dev. 18 (2004) 2368–2379.
556 https://doi.org/10.1101/gad.1231804.
557 [15] S.A. Siddiqui, C. Sarmiento, M. Kiisma, S. Koivumäki, A. Lemmetty, E. Truve, K.
558 Lehto, Effects of viral silencing suppressors on tobacco ringspot virus infection in two

Nicotiana species, Journal of General Virology, 89 (2008) 1502–1508. https://doi.org/10.1099/vir.0.83621-0.

[16] K.R. Kondhare, N.S. Patil, A.K. Banerjee, A historical overview of long-distance signalling in plants, Journal of Experimental Botany 72 (2021) 4218–4236. https://doi.org/10.1093/jxb/erab048.

[17] J.A. Lindbo, W.G. Dougherty, Untranslatable transcripts of the tobacco etch virus coat protein gene sequence can interfere with tobacco etch virus replication in transgenic plants and protoplasts, Virology 189 (1992) 725–733. https://doi.org/10.1016/0042-6822(92)90595-G.

[18] W.G. Dougherty, J.A. Lindbo, H.A. Smith, T.D. Parks, S. Swaney, W.M. Proebsting, RNA-mediated virus resistance in transgenic plants: exploitation of a cellular pathway possibly involved in RNA degradation, Mol Plant Microbe Interact 7 (1994) 544–552.

[19] H.A. Smith, S.L. Swaney, T.D. Parks, E.A. Wernsman, W.G. Dougherty, Transgenic plant virus resistance mediated by untranslatable sense RNAs: expression, regulation, and fate of nonessential RNAs, Plant Cell 6 (1994) 1441–1453. https://doi.org/10.1105/tpc.6.10.1441.

[20] A.M. Koltunow, J. Truettner, K.H. Cox, M. Wallroth, R.B. Goldberg, Different Temporal and Spatial Gene Expression Patterns Occur during Anther Development., The Plant Cell 2 (1990) 1201–1224. https://doi.org/10.1105/tpc.2.12.1201.

[21] A.C. Jackson, Detection of rabies virus mRNA in mouse brain by using in situ hybridization with digoxigenin-labelled RNA probes, Molecular and Cellular Probes 6 (1992) 131–136. https://doi.org/10.1016/0890-8508(92)90057-5.

[22] J.-P. Vielle-Calzada, J. Thomas, C. Spillane, A. Coluccio, M.A. Hoeppner, U. Grossniklaus, Maintenance of genomic imprinting at the Arabidopsis medea locus requires zygotic DDM1 activity, Genes Dev. 13 (1999) 2971–2982.

[23] P. Vargas-Mejía, J. Vega-Arreguín, G. Chávez-Calvillo, E. Ibarra-Laclette, L. Silva-Rosales, Differential Accumulation of Innate- and Adaptive-Immune-Response-Derived Transcripts during Antagonism between Papaya Ringspot Virus and Papaya Mosaic Virus, Viruses 12 (2020) 230. https://doi.org/10.3390/v12020230.

[24] C.D. Fabbro, S. Scalabrin, M. Morgante, F.M. Giorgi, An Extensive Evaluation of Read Trimming Effects on Illumina NGS Data Analysis, PLOS ONE 8 (2013) e85024. https://doi.org/10.1371/journal.pone.0085024.

[25] N.L. Bray, H. Pimentel, P. Melsted, L. Pachter, Near-optimal probabilistic RNA-seq quantification, Nature Biotechnology 34 (2016) 525–527. https://doi.org/10.1038/nbt.3519.

[26] K.D. Edwards, N. Fernandez-Pozo, K. Drake-Stowe, M. Humphry, A.D. Evans, A. Bombarely, F. Allen, R. Hurst, B. White, S.P. Kernodle, J.R. Bromley, J.P. Sanchez-Tamburrino, R.S. Lewis, L.A. Mueller, A reference genome for Nicotiana tabacum enables map-based cloning of homeologous loci implicated in nitrogen utilization efficiency, BMC Genomics 18 (2017) 448. https://doi.org/10.1186/s12864-017-3791-6.

[27] L. Yi, H. Pimentel, N.L. Bray, L. Pachter, Gene-level differential analysis at transcript-level resolution, Genome Biology 19 (2018) 53. https://doi.org/10.1186/s13059-018-1419-z.

[28] T. Tian, Y. Liu, H. Yan, Q. You, X. Yi, Z. Du, W. Xu, Z. Su, agriGO v2.0: a GO analysis toolkit for the agricultural community, 2017 update, Nucleic Acids Res 45 (2017) W122–W129. https://doi.org/10.1093/nar/gkx382.

[29] P. Shannon, A. Markiel, O. Ozier, N.S. Baliga, J.T. Wang, D. Ramage, N. Amin, B. Schwikowski, T. Ideker, Cytoscape: A Software Environment for Integrated Models of Biomolecular Interaction Networks, Genome Res. 13 (2003) 2498–2504. https://doi.org/10.1101/gr.1239303.

[30] F. Supek, M. Bošnjak, N. Škunca, T. Šmuc, REVIGO Summarizes and Visualizes Long Lists of Gene Ontology Terms, PLOS ONE 6 (2011) e21800. https://doi.org/10.1371/journal.pone.0021800.
[31] M.J. Axtell, ShortStack: comprehensive annotation and quantification of small RNA genes, RNA 19 (2013) 740–751. https://doi.org/10.1261/rna.035279.112.
[32] X. Dai, Z. Zhuang, P.X. Zhao, psRNATarget: a plant small RNA target analysis server (2017 release), Nucleic Acids Res 46 (2018) W49–W54. https://doi.org/10.1093/nar/gky316.
[33] R. Zavaliev, B.L. Epel, Imaging Callose at Plasmodesmata Using Aniline Blue: Quantitative Confocal Microscopy, in: M. Heinlein (Ed.), Plasmodesmata: Methods and Protocols, Springer, New York, NY, 2015: pp. 105–119. https://doi.org/10.1007/978-1-4939-1523-1_7.
[34] K.M. Myles, M.R. Wiley, E.M. Morazzani, Z.N. Adelman, Alphavirus-derived small RNAs modulate pathogenesis in disease vector mosquitoes, Proceedings of the National Academy of Sciences 105 (2008) 19938–19943. https://doi.org/10.1073/pnas.0803408105.
[35] B. Ghoshal, H. Sanfaçon, Temperature-dependent symptom recovery in Nicotiana benthamiana plants infected with tomato ringspot virus is associated with reduced translation of viral RNA2 and requires ARGONAUTE 1, Virology 456–457 (2014) 188–197. https://doi.org/10.1016/j.virol.2014.03.026.
[36] A.M. Martín-Hernández, D.C. Baulcombe, Tobacco Rattle Virus 16-Kilodalton Protein Encodes a Suppressor of RNA Silencing That Allows Transient Viral Entry in Meristems, Journal of Virology 82 (2008) 4064–4071. https://doi.org/10.1128/JVI.02438-07.
[37] C.J. Kørner, N. Pitzalis, E.J. Peña, M. Erhardt, F. Vazquez, M. Heinlein, Crosstalk between PTGS and TGS pathways in natural antiviral immunity and disease recovery, Nature Plants 4 (2018) 157–164. https://doi.org/10.1038/s41477-018-0117-x.
[38] M.M. Pooggin, How Can Plant DNA Viruses Evade siRNA-Directed DNA Methylation and Silencing?, International Journal of Molecular Sciences 14 (2013) 15233–15259. https://doi.org/10.3390/ijms140815233.
[39] E. Rodríguez-Negrete, R. Lozano-Durán, A. Piedra-Aguilera, L. Cruzado, E.R. Bejarano, A.G. Castillo, Geminivirus Rep protein interferes with the plant DNA methylation machinery and suppresses transcriptional gene silencing, New Phytologist 199 (2013) 464–475. https://doi.org/10.1111/nph.12286.
[40] F. Di Serio, A.-E. Martínez de Alba, B. Navarro, A. Gisel, R. Flores, RNA-Dependent RNA Polymerase 6 Delays Accumulation and Precludes Meristem Invasion of a Viroid That Replicates in the Nucleus, Journal of Virology 84 (2010) 2477–2489. https://doi.org/10.1128/JVI.02336-09.
[41] H. Garcia-Ruiz, A. Carbonell, J.S. Hoyer, N. Fahlgren, K.B. Gilbert, A. Takeda, A. Giampetruzzi, M.T.G. Ruiz, M.G. McGinn, N. Lowery, M.T.M. Baladejo, J.C. Carrington, Roles and Programming of Arabidopsis ARGONAUTE Proteins during Turnip Mosaic Virus Infection, PLOS Pathogens 11 (2015) e1004755. https://doi.org/10.1371/journal.ppat.1004755.
[42] R. Anandalakshmi, R. Marathe, X. Ge, J.M. Herr, C. Mau, A. Mallory, G. Pruss, L. Bowman, V.B. Vance, A Calmodulin-Related Protein That Suppresses Posttranscriptional Gene Silencing in Plants, Science 290 (2000) 142–144. https://doi.org/10.1126/science.290.5489.142.
[43] F. Li, C. Huang, Z. Li, X. Zhou, Suppression of RNA Silencing by a Plant DNA Virus Satellite Requires a Host Calmodulin-Like Protein to Repress RDR6 Expression, PLoS Pathog 10 (2014). https://doi.org/10.1371/journal.ppat.1003921.

[44] K.S. Nakahara, C. Masuta, S. Yamada, H. Shimura, Y. Kashihara, T.S. Wada, A. Meguro, K. Goto, K. Tadamura, K. Sueda, T. Sekiguchi, J. Shao, N. Itchoda, T. Matsumura, M. Igarashi, K. Ito, R.W. Carthew, I. Uyeda, Tobacco calmodulin-like protein provides secondary defense by binding to and directing degradation of virus RNA silencing suppressors, Proceedings of the National Academy of Sciences 109 (2012) 10113–10118. https://doi.org/10.1073/pnas.1201628109.

[45] F. Kragler, Plasmodesmata: intercellular tunnels facilitating transport of macromolecules in plants, Cell Tissue Res 352 (2013) 49–58. https://doi.org/10.1007/s00441-012-1550-1.

[46] T. Muhammad, F. Zhang, Y. Zhang, Y. Liang, RNA Interference: A Natural Immune System of Plants to Counteract Biotic Stressors, Cells 8 (2019) 38. https://doi.org/10.3390/cells8010038.

[47] T. Wang, X. Li, X. Zhang, Q. Wang, W. Liu, X. Lu, S. Gao, Z. Liu, M. Liu, L. Gao, W. Zhang, RNA Motifs and Modification Involve in RNA Long-Distance Transport in Plants, Front. Cell Dev. Biol. 9 (2021). https://doi.org/10.3389/fcell.2021.651278.

[48] F. Schwach, F.E. Vaistij, L. Jones, D.C. Baulcombe, An RNA-dependent RNA polymerase prevents meristem invasion by potato virus X and is required for the activity but not the production of a systemic silencing signal, Plant Physiol 138 (2005) 1842–1852. https://doi.org/10.1104/pp.105.063537.

[49] A. Medzihradszky, P. Gyula, A. Sós-Hegedűs, G. Szittya, J. Burgyán, Transcriptome reprogramming in the shoot apical meristem of CymRSV-infected Nicotiana benthamiana plants associates with viral exclusion and the lack of recovery, Molecular Plant Pathology 20 (2019) 1748–1758. https://doi.org/10.1111/mpp.12875.

[50] R.B. Anjanappa, D. Mehta, M.N. Maruthi, E. Kanju, W. Gruissem, H. Vanderschuren, Characterization of Brown Streak Virus–Resistant Cassava, MPMI 29 (2016) 527–534. https://doi.org/10.1094/MPMI-01-16-0027-R.

[51] R.B. Anjanappa, D. Mehta, M.J. Okoniewski, A. Szabelska-Beręsewicz, W. Gruissem, H. Vanderschuren, Molecular insights into Cassava brown streak virus susceptibility and resistance by profiling of the early host response, Mol. Plant Pathol. 19 (2018) 476–489. https://doi.org/10.1111/mpp.12565.

[52] A. Molnár, T. Csorba, L. Lakatos, É. Várallyay, C. Lacomme, J. Burgyán, Plant Virus-Derived Small Interfering RNAs Originate Predominantly from Highly Structured Single-Stranded Viral RNAs, Journal of Virology 79 (2005) 7812–7818. https://doi.org/10.1128/JVI.79.12.7812-7818.2005.

[53] D. Nigam, K. LaTourrette, H. Garcia-Ruiz, Mutations in virus-derived small RNAs, Sci Rep 10 (2020) 9540. https://doi.org/10.1038/s41598-020-66374-2.

[54] V. Golyaev, T. Candresse, F. Rabenstein, M.M. Pooggin, Plant virome reconstruction and antiviral RNAi characterization by deep sequencing of small RNAs from dried leaves, Sci Rep 9 (2019) 19268. https://doi.org/10.1038/s41598-019-55547-3.

[55] L. Lakatos, T. Csorba, V. Pantaleo, E.J. Chapman, J.C. Carrington, Y.-P. Liu, V. Dolja, L. Fernández, J.J. López-Moya, J. Burgyán, Small RNA binding is a common strategy to suppress RNA silencing by several viral suppressors, The EMBO Journal 25 (2006) 2768–2780. https://doi.org/10.1038/sj.emboj.7601164.

[56] A.A. Valli, A. Gallo, B. Rodamilans, J.J. López-Moya, J.A. García, The HCPro from the Potyviridae family: an enviable multitasking Helper Component that every virus would like to have, Molecular Plant Pathology 19 (2018) 744–763. https://doi.org/10.1111/mpp.12553.